ATMOSPHERIC MESOSCALE MODELING OF WATER AND CLOUDS DURING NORTHERN SUMMER ON MARS

D. Tyler, *College of Earth Oceanic and Atmospheric Sciences, Oregon State University, Corvallis, OR, USA (dtyler@coas.oregonstate.edu)*, **J. Barnes**, *College of Earth Oceanic and Atmospheric Sciences, Oregon State University, Corvallis, OR, USA,* **B. Cantor**, *Malin Space Sciences Systems, San Diego, CA, USA.*

Introduction: A mesoscale modeling study of the water cycle during northern polar summertime (L_s~120°) has been performed. Although the vapor column in the polar atmosphere has only just started to fall below the annual and global maximum, the mass of water in cloud ice is very near the annual minimum for the region. GCMs have a difficult time with this season (e.g. *Haberle et al.*, 2011; *Madeleine et al*., 2012), predicting too much water mass in the form of cloud ice, and the problem is even worse when the effects of radiatively active clouds (RAC) are included. In the absence of seasonal frost, the northern polar region is incredibly complex, with sharp gradients in ground temperature and all surface properties at scales that are just not resolved in any typical GCM study. Moreover, many operational GCMs are also hindered by the "pole problem", where grid-boxes become highly elongated in the meridional direction near the pole (non-physical filtering is needed for computational stability). Since the northern polar summertime is climatologically important, higher resolution modeling (without these problems) is used to resolve the circulation and understand its role in this issue.

In this study, TES observations are used for model tuning, while MOC and MARCI imagery provide evidence of a circulation as complex as the region itself. Our results suggest that sufficient resolution of the polar region is an important part of solving the problem of too much cloud ice in GCMs.

The data collected by the Phoenix mission (*Tamppari*, 2010) are extremely useful. These data describe meteorological changes that were observed at the lander, and provide a timeline over which these changes occurred during this seasonal period. In comparison with both the Phoenix data and the MARCI imagery at Ls~120° in 2008 (*B. Cantor, personal communication*, 2013), a similar and consistent sequence of events is seen in the model results. An annular cloud, very similar to that observed by *Cantor et al*. (2002), forms in the model. The dynamics that lead to the formation of this recurring phenomenon are being investigated.

The OSU MMM: The Oregon State University Mars Mesoscale Model (OSU MMM) has been used in a number of studies of the atmosphere of Mars, most recently in support of EDL for MSL Curiosity (*Tyler and Barnes*, 2013). Two model modifications are key to this study: 1) a cloud scheme based on that of *Montmessin et al*. (2004), and 2) new albedo and thermal inertia maps for the most poleward latitudes. Details of the cloud scheme and its incorporation are described in *Tyler and Barnes* (2013b). The new surface property maps were constructed using the publically available data of *Putzig and Mellon* (2007) and composite MARCI imagery (*W. Calvin, personal communication,* 2009). In an iterative process, the albedo and thermal inertia maps were tuned so model ground temperatures were in very good agreement with TES (for both AM and PM times) for this season. The final albedo map is shown in Fig. 1.

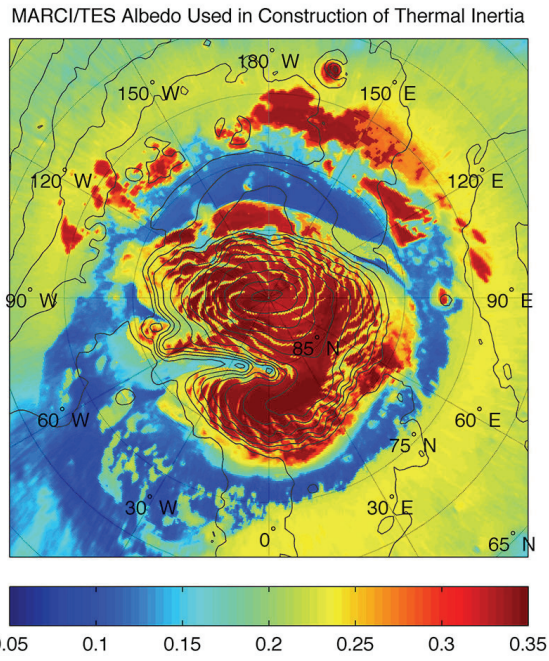

Figure 1. A map of the constructed albedo field is shown. These data are the result of in an iterative process that combined MARCI imagery and the results of *Putzig and Mellon* (2007).

The OSU MMM is run on a polar stereographic map projection. Two levels of nesting are used to reach a spatial resolution of 15 km for the polar region. There are 55 model layers in the vertical, with the model top at 0.01 Pa. The model is run for a total of 30 sols, with the final 20 sols centered on L_s~120°. Initial and boundary conditions are provided by a version of the NASA Ames GCM (as maintained at OSU). Throughout the simulation, the zonal-mean vapor column depths remain in very good agreement with TES, a consequence of two factors: 1) realistic boundary conditions and initialization, and 2) realistic sublimation rates from NPRC

ices. A simulation of this duration is not long enough to "spin up" a vapor distribution, although there is plenty of time for it to diverge greatly from the initial state.

Results: Numerous simulations were used to investigate the sensitivity of water ice clouds over the polar region to the number of ice nuclei (dust particle number density). Using our best-case prescription, a low-resolution (no nests) case is compared to show the importance that spatial resolution has on polar cloudiness. Finally, in relation to a rapidly evolving circulation on the poleward slopes of Alba Patera, the formation of an annular cloud is described in the context of MARCI and Phoenix observations.

Cloud scheme sensitivity to dust. The vertical profile of the dust particle number density (used in the cloud scheme) is consistent with the dust opacity as prescribed for atmospheric radiation. We assume nominally that 50% of the dust particles become cloud particles in favorable conditions. With the prescribed dust distribution, model air temperatures are in good agreement with TES, although too much cloud ice forms over the polar region when this 50% value is prescribed globally. A suite of experiments was performed, where the fraction of dust particles that can become ice nuclei (f_{IN}) varies with latitude. The case that best agrees with opacity observations has f_{IN} decreasing from 50% to 5% between ~60° N and ~80° N. Another case, which limits f_{IN} more strongly, decreases to ~5% at the latitude of Phoenix and to ~2.5% by ~75° N [these lowest fractional values are in good agreement with the ~3% values reported by *Daerden et al*. (2010)]. In this stronger limiting case, cloud ice opacities become too small at high latitudes, although cloud particles over Phoenix grow much larger and fall nearer to the ground in the early AM, in better agreement with the LIDAR observations (*Whiteway et al*., 2009).

This sensitivity study suggests that cloud formation can be roughly grouped into two categories: 1) clouds that form in environments with large diurnal cycles and strong dynamics (with larger supersaturations), and 2) clouds that form in environments with much smaller diurnal cycles and smaller supersaturations. In the second case, the larger dust particles would nucleate and grow large at the expense of the smaller particles being able to nucleate. In the first case, the larger supersaturation values would allow many smaller dust particles to nucleate at the same time as the larger ones. As a result, values of f_{IN} will differ greatly between the two cases. Any effort to prescribe this variation would be difficult to base in physical reality, which suggests that careful consideration of the nucleation phase must be a key aspect of future modeling efforts.

Spatial resolution and polar clouds. Since the polar region is so complex, with sharp gradients in surface properties as well as ground temperatures, strong and smaller-scale circulations are expected to be an integral part of the regional circulation. Sufficient spatial resolution is needed, and it may be the case that smaller-scale circulations have an important role in the formation of water ice clouds at L_s~120°. By comparing results from two simulations (identical except for resolution), the effect that resolution has on polar cloudiness can be investigated.

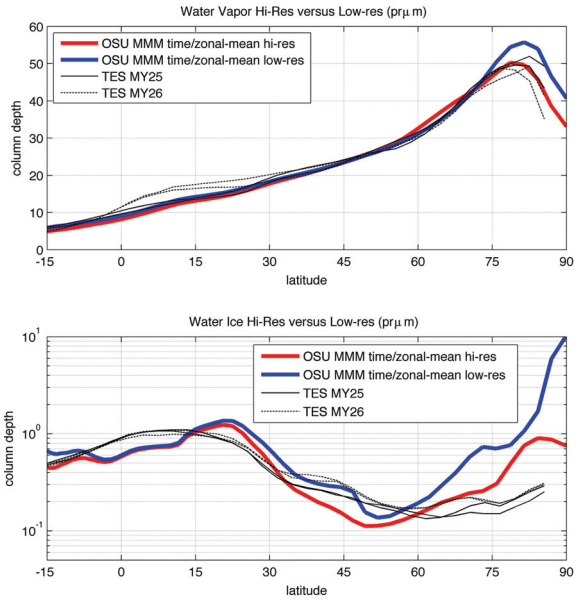

Figure 2. The zonal-mean vapor and water ice column depths are shown for two simulations, the low-resolution (blue) and high-resolution (red) cases. In the lower subplot, ice column depth profiles are compared to an estimate based on PM TES IR opacity data (*M. Smith, personal communication*, 2008).

Using the best-case f_{IN} prescription as described above, a case with nests (15 km resolution) is compared to a case with no nests (135 km resolution). In Fig. 2 the zonal-mean water vapor and ice column depths are shown (as ten sol averages centered on L_s=120°). In the TES PM time comparison of the lower subplot, the low-resolution case has ~10 times more cloud ice over the pole. The upper subplot shows more water vapor over the polar region in the low-resolution case, although this is not a consequence of greater sublimation. There is in fact ~26% more sublimation in the high-resolution case from NPRC ices. The relationship between the circulation and the locations where sublimation of ice happens is key. In the high-resolution case, the smaller-scale aspects of the regional circulation become resolved. The greatest sublimation rates occur near the edges of the largest ice regions, which is also where strong winds and transient circulations are very effective at ventilating vapor equatorward. Spatial resolution has a very important effect on the gradients in the complex polar region in northern

summertime; the katabatic flow off the polar dome, the transient circulations and the strong circumpolar flow become resolved. The central part of the polar dome (and some of the other large ice regions) is actually a region of net diurnal deposition (*Tyler and Barnes*, 2011). Without sufficient resolution, these aspects of the circulation cannot be simulated realistically, suggesting that sufficient resolution is needed to address the GCM cloudiness problem.

Importantly, it is the activation of the first nest (45 km resolution) that causes the sharp reduction in the polar water ice column. For dynamics, a 45 sec timestep is used in the mother domain (135 km), with a 15 sec timestep in the first nest. In this study two sub-timesteps are used for microphysics. GCMs see real improvement when sub-timesteps are used in the microphysics calculations (*Urata et al*., 2013). When the first nest activates in the model, the microphysics timestep becomes smaller than that used by Urata et al., (2013), suggesting the solution to the excessive cloudiness problem is two-fold.

The recurring annular cloud. In a zonal-mean sense, the modeled vapor distribution for L_s~120^o can be seen as constant in time (in good agreement with TES). However, when the specific region between Alba Patera and the polar dome is examined (a region that includes Phoenix), important trends are seen. Changes in the spatial distribution of vapor occur in relation to a circulation that forms on the poleward slopes of Alba Patera; this circulation evolves with time across the L_s~120^o season. The model responds to this circulation and produces results that are in good agreement with the MARCI and Phoenix observations of 2008.

The circulation appears to be caused by a number of dynamical factors that are themselves all affected by seasonal change in the insolation: 1) a large scale thermal circulation, 2) western boundary current flows, and 3) large-scale slope flows. In combination, these forcings presumably give rise to a convergence zone that forms on the northern slopes of Alba Patera. Strong flow, that reaches the most polar latitudes, is associated with this circulation. Transient eddies form along the convergence zone, where the advection of vorticity (produced at the Alba Patera summit) may be involved. With the convergence zone moving eastward, and the existence of transient disturbances, the region is a "storm zone" in the sense that there is a great deal of meteorological variability (*Tyler and Barnes*, 2005).

As the storm zone moves eastward, its northernmost extent advances towards the polar dome. A perturbation develops along the convergence zone that grows into a large transient eddy. It is not clear what triggers the perturbation, although interaction between the convergence zone moving eastward and the strong flow that is seen to wrap around the topography of Tharsis may be involved. The storm zone is also a boundary between two distinct wind environments, with far more transient activity to the east than the west. It is also a transition for CBL depths. It is not a shallow feature in the atmosphere. Its existence does seem to be short-lived during the L_s~120^o season, and it could be the case that only one large transient is generated annually.

The large transient grows and migrates poleward to interact with the flow around the polar dome and the greatest vapor column depths in the region. Its arrival causes changes in the vapor field that favor the formation of an annular cloud. In Fig. 3, the circulation is depicted seven days before the annular cloud forms with a color plot of the diurnal mean wind speed at ~1 km AGL.

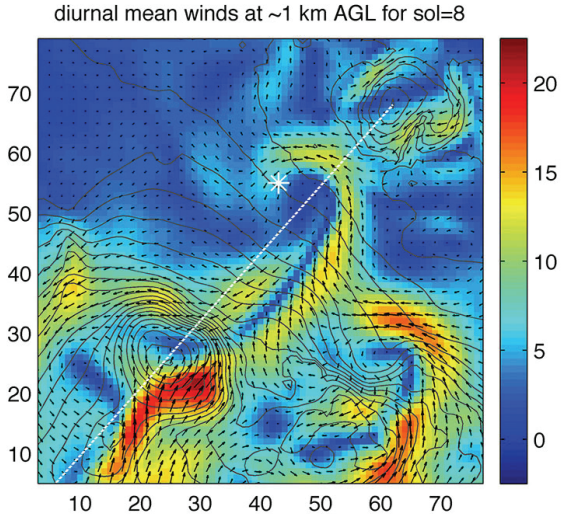

Figure 3. A color map of diurnal mean wind speed at ~1 km AGL is shown for a subset of the 45 km nest (vectors at every other grid point show wind direction). Topography is contoured (Alba Patera is at the bottom left and the polar dome is at the upper right). A white asterisk marks Phoenix.

Before the large transient develops, the flow contributes in keeping the atmosphere over Phoenix drier than the zonal-mean vapor column value. Dry air is advected into the region from the south; the circulation is also very effective at ventilating vapor (sublimated from ices) off to the southwest of Phoenix. The circulation may impede the formation of transients that would be effective at bringing moist air over Phoenix. As the circulation evolves, the diurnal mean winds begin to wrap, leading to the advection of water vapor (that was being advected to the southwest) back over Phoenix. This atmospheric state is beginning to develop in Fig. 3. Later, when the large transient enters the Phoenix region, the vapor field becomes tightly wrapped upon itself, much like a frontal occlusion. This is when the annular cloud structure is most clearly seen in the model results. For an early morning time in the 15 km nest (second nest), this annular cloud state is shown in the vapor and ice column fields of Fig. 4.

As seen in MARCI imagery taken during the Phoenix mission, the annular cloud first formed on September 3, 2008 at L_s=121.9° (*B. Cantor personal communication*, 2013). In an interruption to an otherwise highly linear trend in the surface pressure record, Phoenix was affected by a strong transient disturbance at the same time. The effect is centered on L_s=120° (sol #94) with a fractional amplitude of ~1%. In the OSU MMM, the amplitude of the large transient associated with the annular cloud is similar, although the amplitude at Phoenix specifically is not as large as observed. Another change observed at Phoenix in this timeframe was the rapid decrease in the height of AM clouds (to ~4 km AGL). Previously clouds only formed above ~10 km. In the model, after the increase in the vapor column due to changing dynamics, a similar and rapid decrease in the height of cloud ice above the ground in the AM was simulated, with cloud heights dropping from ~10 km to ~5 km AGL. The similarity between model results and observations is encouraging.

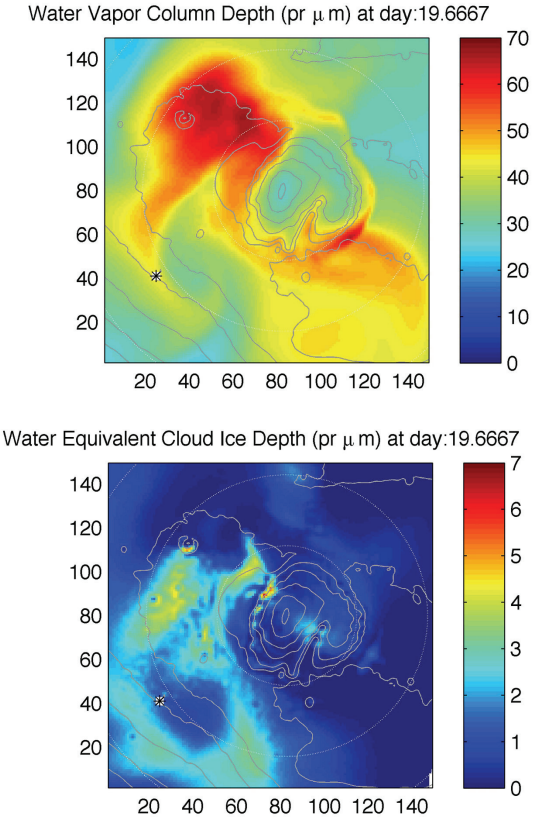

Figure 4. OSU MMM vapor and ice column depths are shown at L_s~124° for the 15 km nest. An annular cloud is seen in the ice column depths. The location of Phoenix is identified with an asterisk in each subplot.

Future Work: In future studies, a more sophisticated cloud scheme will be needed. The fractional nucleation issue (f_{IN}) must be addressed with a carefully considered nucleation phase. This will require some freedom in the dust prescription. A semi-interactive dust prescription (where the dust particle number density is relaxed to a nominal distribution) will be used. Besides the climatological importance of the L_s~120° season, this season poses many unique challenges for modeling studies. It will be important to revisit the hypotheses formed in this study with a more sophisticated model.

References:

Cantor, B. et al., 2002, Multiyear MOC observations of repeated Martian weather phenomena during the northern summer season, *J. Geophys. Res.*, 107(E3), 5014, 10.1029/2001JE001588.

Daerden, F. et al., 2010, Simulating observed boundary layer clouds on Mars, *J. Geophys, Res.*, 37(L04203), 10.1029/2009GL041523.

Haberle, R. et al., 2011. Radiative effects of water ice clouds on the Martian seasonal water cycle. *4th Int. Conference on the Mars Atmosphere: Modeling and Observations*, Paris.

Madeleine, J. et al., 2012. The influence of radiatively active water ice clouds on the Martian climate. *GRL*, 39(L23202), 10.1029/2012GL053564.

Montmessin, F. et al., 2004. Origin and role of water ice clouds in the martian water cycle as inferred from a General Circulation model. *J. Geophys. Res.*, 109(E10004), 10.1029/2004JE002284.

Putzig, N., M. Mellon, 2007. Apparent thermal inertia and the surface heterogeneity of Mars. *Icarus*, 191, 68-94, 10.1016/j.icarus.2007.05.013.

Tamppari, L., 2010. Phoenix and MRO coordinated atmospheric measurements. *J. Geophys. Res.*, 115(E00E17), 10.1029/2009JE003415.

Tyler, D., J. Barnes, 2005. A mesoscale model study of summertime atmospheric circulations in the north polar region of Mars. *J. Geophys. Res.*, 110(E06007), 10.1029/2004JE002356

Tyler, D., J. Barnes, 2011, Atmospheric mesoscale modeling of water and clouds in northern summer. *5th Mars Polar Sci. Conf.*, Fairbanks, AK, #6049.

Tyler, D., J. Barnes, 2013. Mesoscale modeling of the circulation in the Gale Crater region: an investigation into the complex forcing of CBL depths, *Mars 8*, 58-77, 10.1555/mars.2013.0003.

Tyler, D., J. Barnes, 2013b. Atmospheric mesoscale modeling of water and clouds during northern summer on Mars, *Icarus*, *in review*.

Urata, R. et al., 2013. Timescales are short for the formation of water ice clouds on Mars, *45th DPS Meeting*, October 9, 2013, Denver, CO, 313.06.

Whiteway, J. et al., 2009. Mars water ice clouds and precipitation. *Science*, 325, 68-70, doi: 10.1126/science.1172344.